



Morpho-densitometric traits for quinoa (*Chenopodium quinoa* Willd.) seed phenotyping by two X-ray micro-CT scanning approaches

Laura Gargiulo^a, Åsa Grimberg^b, Ritva Repo-Carrasco-Valencia^c, Anders S. Carlsson^b, Giacomo Mele^{a,*}

^a Institute for Agricultural and Forest Systems in the Mediterranean-National Research Council, ISAFOM-CNR, Via Patacca 85, 80056, Ercolano, Italy

^b Department of Plant Breeding, Swedish University of Agricultural Sciences, Sundsvägen 10, 23052, Alnarp, Sweden

^c Centro de Investigación e Innovación en Productos Derivados de Cultivos Andinos, CIINCA, Universidad Nacional Agraria La Molina, Avenida La Molina S/n Lima 12, Peru

ARTICLE INFO

Keywords:

X-ray micro-CT
Quinoa
Seed quality
3D image analysis

ABSTRACT

Recent studies are increasingly focusing on quinoa (*Chenopodium quinoa*) as a high-quality protein-rich food source and, in general, on seed quality. This latter is a complex trait difficult to characterize with standard measurements or analyses.

X-ray micro-CT allows to visualise the internal structure of small objects and has been already used in seed research, mostly for maize kernel characterization. To date this technique has not yet been applied to study quinoa seeds, despite the increasing interest for their nutritional properties.

The aim of this work was to explore the use of X-ray microtomography to provide new traits improving the seed phenotyping of quinoa. Two different scanning approaches have been compared: one based on the simultaneous scanning of multiple seeds (30) at lower resolution (20 µm voxel size) and one based on the scanning of a single seed at higher resolution (2 µm voxel size). Such approaches were tested on a study case consisting of four different quinoa genotypes.

Among the measured morpho-densitometric parameters, the embryo volume and weight ratios (derived from bulk and single seed scanning, respectively) showed high positive correlation with the total protein content, while the thickest fraction of the pericarp was the best correlated with the presence of saponins.

1. Introduction

Native to South America, quinoa (*Chenopodium quinoa* Willd.) has become a popular food in the last 20 years in Europe and North America (Ruiz et al., 2017), thanks to its high nutritional value and its great adaptability (Hinojosa et al., 2018). Quinoa is a seed crop with increasingly high interest as high-quality protein-rich food source. It plays a key role in the protein transition from animal-based protein to plant-based protein with clear impact on reduction of carbon footprint. Moreover quinoa seeds are gluten-free, have a low glycemic index, contain fiber, lipids, carbohydrates, vitamins and minerals (Jarvis et al., 2017).

Quinoa can be grown on marginal lands and its adaptation to new environments has been shown to be very fast as compared to many other crops (Jacobsen, 2017).

Commercial production of quinoa is rapidly increasing and the potential of using quinoa in the food and healthcare sector is huge

(Fuentes and Paredes-Gonzales, 2015). According to the FAO, quinoa is regarded as a new world staple and predicted to spread fast across the globe (FAO & CIRAD, 2015).

Breeding programs in quinoa have mainly focused on the development of better environmentally adapted varieties (Bazile et al., 2016; Zurita-Silva et al., 2014) and less attention has been paid to the seed nutritional properties.

However, the improvement of quinoa seed quality is challenging and key for food security (Reguera et al., 2018). The quality of the seeds is a complex trait that results from the interaction of genetic and environmental factors (Wimalasekera, 2015). Recent studies have investigated the nutritional properties of quinoa seeds of many genotypes and the effects of different agro-environmental growth conditions (Reguera et al., 2018; Wu et al., 2016; Prado et al., 2014).

Localization of the main seed storage compounds inside the seeds of quinoa is known to have a marked compartmentation. Proteins are located mostly in the embryo (57% of total protein in the whole grain),

* Corresponding author.

E-mail address: giacomo.mele@cnr.it (G. Mele).

<https://doi.org/10.1016/j.jcs.2019.102829>

Received 13 May 2019; Received in revised form 4 September 2019; Accepted 4 September 2019

Available online 06 September 2019

0733-5210/ © 2019 The Authors. Published by Elsevier Ltd. This is an open access article under the CC BY-NC-ND license

(<http://creativecommons.org/licenses/by-nc-nd/4.0/>).

while carbohydrate reserves (starch) are located principally in the perisperm. The pericarp holds 86% of the total saponin amount in seeds (Prego et al., 1998; Ando et al., 2002). In particular, Van Raamsdonk et al. (2010) showed that the saponins are predominantly present in the papillose cells of the pericarp. Although saponins are bitter antinutritional compounds, they have found wide application in pharmaceutical and biopesticides production (Yao et al., 2014; Liu et al., 2013; Ruiz et al., 2017).

Nowadays X-ray micro-computed tomography (microCT) and three-dimensional (3D) image analysis have been successfully applied in food science and seed research because it is a non-destructive and non-invasive approach, which allows to directly visualise and morphometrically characterize the whole seed and its anatomy including internal microstructural features (parts or tissues). X-ray microCT has been used for maize kernel characterisation (Carvalho et al., 1999) to distinguish the major internal anatomical features (Takhar et al., 2011), to determine volume and density (Gustin et al., 2013) and maize hardness using a density calibration (Guelpa et al., 2015).

To the best of our knowledge, X-ray microtomography has never been used for the study of quinoa grains. Only 2D image analysis has been employed to determine morphological and color features of quinoa seeds in order to identify the geographical provenance of different varieties (Medina et al., 2010) or to discriminate different colored quinoa seeds (Abderrahim et al., 2015). Moreover, some works carried out to determine the geometric properties of quinoa seeds useful for industrial seed processing have still been based on the use of the micrometer (Altuntas et al., 2018; Vilche et al., 2003). Furthermore, until now the characterization of the seed external and internal structure and the measurement of some micromorphological features, such as the seed coat thickness (e.g. Jarvis et al., 2017), have been carried out only by means of scanning electron microscopy (Rizvi et al., 2017) on very small sections.

The aim of this work was to compare two different approaches of X-ray microtomographic scanning of quinoa grains, which provide morpho-densitometric characterisation of the seed and its different parts, in order to determine novel traits useful for phenotyping this crop. Namely, we compared results obtained from the scanning of multiple seeds at one time with those achieved from the scanning of one seed at a time and investigated their correlation to two main quinoa seed nutritional parameters, total protein content and saponin amount.

2. Experimental

2.1. Quinoa genotypes and growth conditions

Four different varieties of quinoa were used in this work: INIA 415-Pasankalla and INIA 431-Altiplano selected by INIA, the Peruvian Institution of Agronomic Innovation (<http://www.fao.org/3/a-i4596e.pdf>), Regalona Baer (<https://semillasbaer.cl>) from Chile and a Titicaca cultivar from Europe developed by a Danish breeder (www.quinoaquality.com).

Quinoa seeds were surface sterilized by first shaking in 70% EtOH (10 min) followed by 50% hypochlorite solution (60 min) and then rinsed three times in distilled water. Seeds were sown at a depth of 2 cm in 3.5 L pots in potting soil enriched with solid fertilizer (Basacote Plus 3M). Germinated seedlings were reduced to one plant per pot. Plants were grown in controlled growth chambers (Biotrone, SLU-Alnarp) under fluorescent light ($300 \mu\text{mol m}^{-2}\text{s}^{-1}$ photosynthetically active radiation), under a 12/12 h light/dark photoperiod at 20/17 °C temperature and 70% humidity. Seeds were harvested from three biological replicates (three individual plants) at maturity and threshed manually. It should be noted that the onset of flowering (and therefore also seed harvest) differed between the varieties, probably due to variety differences in day length sensitivity. Threshed seeds were stored in paper bags in room temperature until further analyses.

2.2. Protein content

Approximately 1.5 mL threshed mature seeds were ground with a steel bead ($d = 16 \text{ mm}$, 30 Hz, $4 \times 15 \text{ s}$) in a mixer mill in 35 mL stainless steel containers (Retsch). Seed flour was stored at $-20 \text{ }^\circ\text{C}$ and then freeze dried for 48 h. Amounts of $4 \pm 0.2 \text{ mg}$ of freeze dried seed flour were weighed into tin capsules on a microbalance (Mettler Toledo XP6). The capsules were folded and all air pressed out and placed in an autosampler for introduction into an elemental analyzer (Flash 2000; Thermo Scientific) together with a small amount of oxygen for burning at $1800 \text{ }^\circ\text{C}$ in an oxidation column. Produced NO_x was further reduced to N_2 (g) in a reduction column and separated from CO_2 on a molecular sieve packed GC column and analyzed with a thermal conductivity detector. Data was analyzed using Eager Xperience software (ver 1.2, Thermo Scientific) to determine total N content, and total protein content was further estimated as total N $\times 6.25$.

2.3. Saponin content

An afrosimetric method was used to get an estimation of the saponin content of the chosen quinoa genotypes. It is based on the correlation among the foam height formed under specific conditions and the total amount of saponins. The presence of saponins in quinoa grains is visible after vigorous shaking in aqueous buffered solutions and can be reproducibly measured by following exact timing, amounts and tube sizes. The standard procedure described by Koziol (1991) was used here. Quinoa seeds ($0.50 \pm 0.02 \text{ g}$) were weighed directly into a screwcap test tube (160 mm long, 16 mm diameter). Upon the addition of 5 ml of distilled water the tube was capped and shaken vigorously (4 shakes s⁻¹, up and down movement) for 30 s. After two successive rests of 30 min, the tube was shaken vigorously for 30 s. After a rest of 5 min the foam height was read to the nearest 0.1 cm. Such a protocol was repeated on three seed samples for each genotype.

2.4. X-ray microCT

The X-ray microCT scans were performed using the microtomograph Skyscan 1272 (<http://bruker-microct.com/products/1272.htm>) available at the National Research Council of Italy - Institute for Agricultural and Forest Systems in the Mediterranean in Ercolano (Italy). It is a desktop microtomograph with a cone beam X-ray source adjustable in the 20–100 kV energy range which allows a cylinder shaped volume of 6.5 cm in diameter and 7.2 cm height as maximum sample size.

As there are no standard procedures for seed micro CT scanning and analysis, multiple scanning and image analysis tests were performed trying different settings before reaching the final setup for the two scanning and analysis protocols described below.

2.4.1. Bulk seed scanning

Before the X-ray microCT scanning, 30 seeds for each genotype were randomly selected, 10 for each plant, discarding to the stereomicroscope those with damaged or incomplete pericarp. Each seed was weighted using a digital electronic balance (0.001 g resolution).

All 30 seeds for each genotype were acquired in one time arranging them in a PMMA cylinder of 2.5 cm diameter whose internal surface was coated with a polystyrene film. The height of the cylinder was 2.8 cm and contained three superimposed polystyrene thin discs having small depressions containing ten seeds each. PMMA material for the cylinder and the polystyrene for the discs were chosen because of their low X-ray attenuation capacity, allowing good contrast in the imaging of the seeds. The main function of the discs with the housings for the seeds is to obtain an image where seeds do not touch each other, thus simplifying the following stage of image processing. Image acquisition was set at a source voltage and current of 50 kV and 200 μA , respectively. X-ray scans were acquired at 20 μm voxel size and required

approximately 10 min to complete.

2.4.2. Single seed scanning

Because the sample size affects the resolution at which images can be acquired and thus the seed parts which can be identified and segmented, for the characterization of the pericarp thin structure single seeds of each genotype were scanned separately at higher resolution. One seed at a time was directly put on the rotating stage of the microtomograph using a very thin support to which the seed was held using dental wax. Such dental wax is suitable for the purpose because of its very low x-ray attenuation coefficient.

Source voltage and current were set at 50 kV and 200 μ A respectively as above, but X-ray scans were acquired at 2 μ m voxel size thanks to the geometric magnification allowed by the short distance seed to source in this case. Each scan took approximately 20 min to complete. Three seeds for each genotype were singularly scanned after being weighted with digital electronic balance.

2.5. Image processing

The series of two-dimensional X-ray projection images obtained from the micro-CT scans were reconstructed in a 3D image using the NRecon software, version 1.7.3 (www.bruker-microct.com). The reconstruction procedure comprised a filtered back projection algorithm (Xiao et al., 2003). In order to obtain a proper 3D reconstruction of the images ring artifact and beam hardening corrections were both applied at 30% level for the bulk seed scans and at 30% and 50% levels for the single seed scans, respectively.

The images were binarised applying different thresholds to the gray level histograms in order to segment each different seed part. In particular, images from the bulk seed scans have allowed to segment the whole seed and the embryo of each seed, while also pericarp and perisperm were segmented on images from the single seed scans. Fig. 1 shows examples of reconstructed sections, their histograms and the segmented seed parts from bulk and single seed scans.

In order to assure a direct relationship between X-ray attenuation coefficients and the gray levels of the 3D reconstructed images, the conversion from the projection images to the reconstructed images was performed using the same attenuation coefficient range (0–0.075 and 0–0.2 for bulk and single scans, respectively) for all the samples. As the X-ray attenuation coefficient relates to the density of the acquired material (e.g.: Bush et al., 2005), the ratio between the mean gray values of two seed parts is equal to the ratio between their densities. The mean gray value of each seed part was identified as the mean value of the portion of the gray level histogram corresponding to that seed part (see histograms in Fig. 1), using the CTAn software.

2.6. Image analysis

The segmented images were used to measure volumetric, morphological and densitometric characteristics of the whole seed and of the different seed parts.

Quantification of volumetric and morphological traits was performed on the reconstructed images by applying the so-called “object-based image analysis” approach. It allowed the determination of morphometry of the whole seeds and of the different seed parts, treated as isolated objects segmented from the image background, as described previously. This approach was applied using the software “Image Pro Premier 3D” (www.mediacy.com).

In particular, from the bulk seed scans, the volume, the maximum Feret diameter, the minimum Feret diameter, the Feret diameter ratio of the whole seed, and also the volume of the embryo, were determined for each seed.

From the single seed scans, the volumes of the solid phase of the whole seed and of each seed part (embryo, pericarp and perisperm) were determined after the image segmentation using the same software

as above.

For the characterization of the structure of the pericarp, its thickness distribution was calculated from the binarised images of the segmented pericarp, applying mathematical morphology operators of CTAn software (www.bruker.com) based on the distance transform. Such approach allowed to classify the whole volume of pericarp in three different classes of thickness (as it is shown in Fig. 2a and 2b) and, finally, to quantify the percent volume of pericarp of each thickness class, (Fig. 2c).

2.6.1. Determination of the densities of the seed parts

The densities of the different seed parts (pericarp, embryo and perisperm) were calculated for all the seeds of each genotype, which were scanned with the single seed scanning approach. For this purpose the following equations:

$$W_{tot} = W_{pc} + W_e + W_p$$

$$d_e/d_{pc} = W_e/V_e * V_{pc}/W_{pc}$$

$$d_{pc}/d_p = W_{pc}/V_{pc} * V_p/W_p$$

Were solved for each seed in order to obtain the separate weights of the three seed parts, which are the three unknown variables. In the above equation W, d and V are weight, density and volume, respectively; the subscripts pc, e and p indicate pericarp, embryo and perisperm, respectively. The total weight W_{tot} of each seed and the ratios between the densities of the different seed parts, which were calculated using the mean gray level values of the different seed parts determined from histograms of the images of the single seed scans (see Fig. 1), are known terms, along with the volumes of embryo, perisperm and pericarp.

2.6.2. Morpho-densitometric traits

The following parameters were defined as novel morpho-densitometric traits to phenotype the quinoa seeds: the “embryo ratio” calculated as volume ratio between embryo and whole seeds as determined from bulk seed micro-CT scans; the “pericarp”, “embryo” and “perisperm ratio” calculated as ratios between volume of each of these seed parts and the volume of the solid phase of the seeds; the “pericarp”, “embryo” and “perisperm weight ratio” calculated as weight ratios between each of these seed parts and the whole seeds. The last six parameters are based on measures obtained from single seed micro-CT scans.

2.7. Statistical analysis

The principal component analysis (PCA) on all the measured traits was performed using the software SigmaPlot version 13.0 (www.systatsoftware.com). The same software was used to perform Anova and Fisher LSD tests at a significance level of 0.05 to check differences in the results among the four considered quinoa genotypes. Significance level was set at 0.10 for the Pearson correlation coefficients between all calculated traits.

3. Results

The average values and the standard errors of all phenotypic traits determined for the four quinoa genotypes are reported in Table 1. Complete results are provided in Supplementary Tables.

3.1. Protein and saponin content

The four studied quinoa genotypes were characterized by different protein content. In particular Altiplano showed highest protein content (20.80%), followed by Pasankalla (20.06%), and Regalona (18.03%). Titicaca was the genotype with lowest protein content (15.4%). The

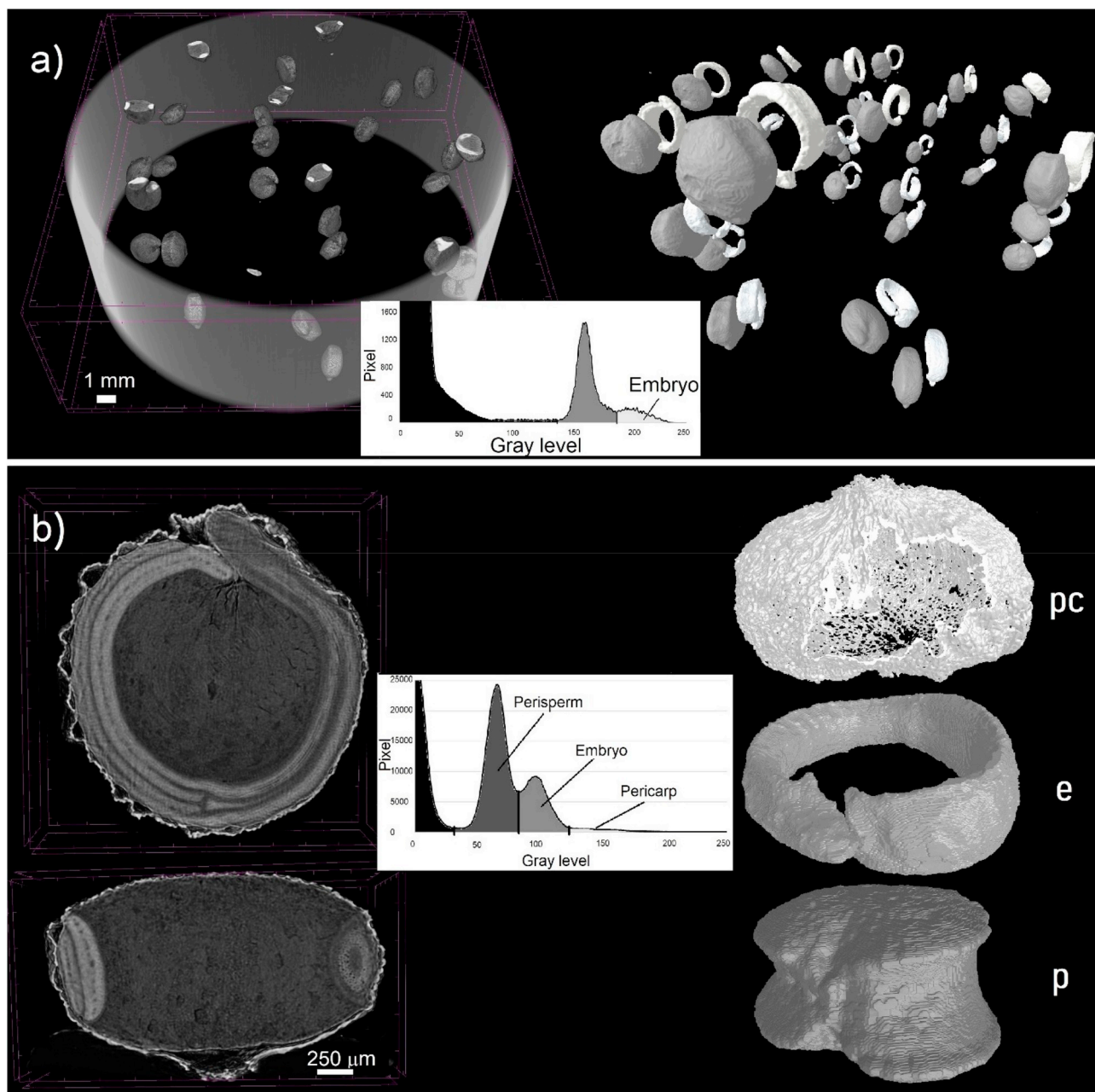


Fig. 1. Three-dimensional reconstructions of quinoa seeds (variety Regalona) and visualisation of their different parts. a) three-dimensional reconstruction and section of a 30 seed sample (left) and virtual separation of embryos from the seeds (right); b) transversal and longitudinal sections of a three-dimensional reconstruction of one seed (left) and visualisation of pericarp (pc), embryo (e) and perisperm (p) volumes (on the right). The graphs in the middle are the gray level histograms of the reconstructed images whose colored areas correspond to the different parts of the seed. The following is a link to see an animation related to this figure: https://youtu.be/zGln_1VCdg?t=83.

protein content of Altiplano and Pasankalla was significantly different from that of Titicaca.

The afrosimetric method used for the estimation of saponin content showed that Altiplano had a foam height (5.5 cm) significantly higher than the others, while the difference between Titicaca and Regalona was not significant (1.7 and 1.8 cm) and Pasankalla had a significantly lowest height (0.3 cm).

Regarding the seed weight, Altiplano showed the highest, followed by Titicaca, Regalona and Pasankalla. Seed weights were significantly different between the genotypes, except for the two combinations of Regalona (3.63 mg) vs Pasankalla (3.50 mg) and Titicaca (4.05 mg) vs Altiplano 4.16 mg).

3.2. Bulk seed scans

In the upper part of Table 1 are reported the results obtained from the bulk seed scans.

Altiplano showed the highest seed volume, followed by Titicaca, Regalona and Pasankalla. All seed volumes were significantly different between genotypes, except for the combinations of Regalona (2.85 mm^3) vs Pasankalla (2.72 mm^3) and Titicaca (3.21 mm^3) vs Altiplano (3.43 mm^3).

Regarding the seed density, Pasankalla showed the highest value (1.28 g/cm^3), followed by Regalona (1.27 g/cm^3), Titicaca (1.26 g/cm^3) and Altiplano, which showed the lowest value (1.21 g/cm^3). Only the seed density of Altiplano was significantly different from all the other

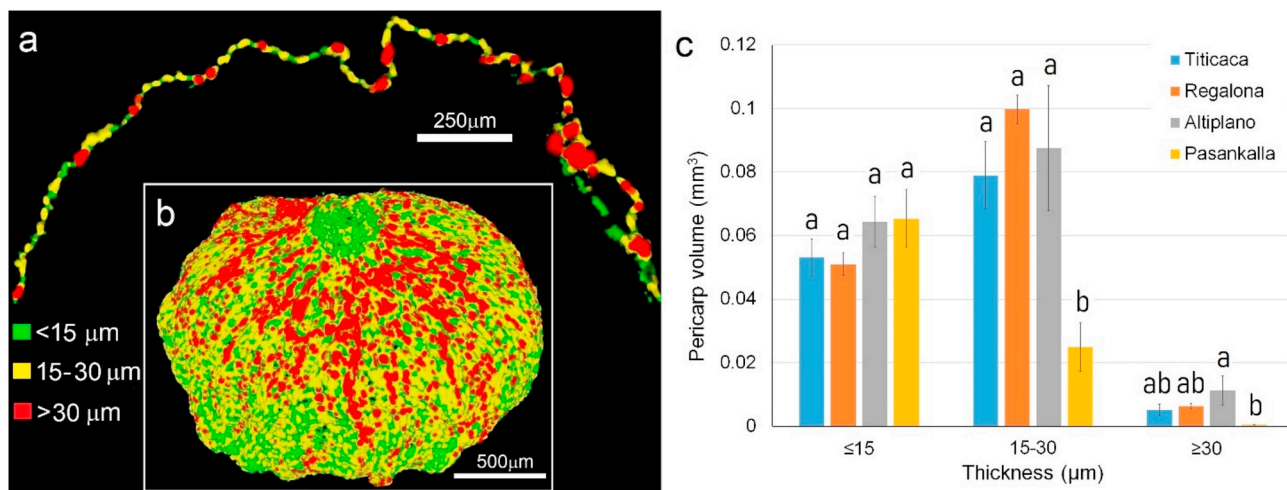


Fig. 2. Pericarp structure characterization. (a) Graphic example of the classification of the pericarp volume in three thickness classes shown in a two-dimensional section and (b) in the entire three-dimensional volume of the pericarp. (c) Pericarp thickness distribution. The mean volumes of pericarp for each thickness class are shown on the y axis. Bars indicate standard errors. Means sharing a letter are not statistically different (*t*-test) at a *P* < 0.05.

genotypes.

Altiplano showed the highest maximum Feret diameter (2.42 mm), followed by Pasankalla (2.34 mm), Titicaca (2.33 mm) and Regalona (2.17 mm). Only the values of Titicaca and Pasankalla were not significantly different.

Altiplano and Pasankalla showed the same Feret diameter ratio (1.98) followed by Titicaca (1.75) and Regalona (1.61). The values of Altiplano and Pasankalla were not significantly different.

The embryo volume ratios of Pasankalla (0.284) and Altiplano (0.280) were almost the same and higher than Regalona (0.247) and Titicaca (0.238). The values of Altiplano and Pasankalla were significantly different as compared to those of Titicaca and Regalona.

3.3. Single seed scans

In the lower part of Table 1 are reported the results obtained from

Table 1

Average values of the seed phenotypic traits and standard errors (in brackets) for the four quinoa genotypes. Means within a same line sharing a letter are not statistically different (*t*-test) at a *P* < 0.05.

Traits		Genotypes				
		Titicaca	Regalona	Altiplano	Pasankalla	
	^b Protein content (% by DW ^a)	15.3(0.8)b	18.0(0.9)ab	20.8(2.1)a	20.1(0.1)a	
	^b Foam height (cm)	1.7(0.2)b	1.8(0.2)b	5.5(0.7)a	0.3(0.1)c	
	^c Seed weight (mg)	4.05(0.11)a	3.63(0.07)b	4.16(0.17)a	3.50(0.08)b	
Bulk seed scan ^c	Seed volume (mm ³)	3.21(0.07)a	2.85(0.06)b	3.43(0.15)a	2.72(0.05)b	
	Seed Density (g/cm ³)	1.26(0.01)a	1.27(0.01)a	1.21(0.00)b	1.28(0.00)a	
	Feret max (mm)	2.33(0.018)b	2.17(0.014)c	2.42(0.029)a	2.34(0.016)b	
	Feret ratio	1.75(0.01)b	1.61(0.01)c	1.98(0.03)a	1.98(0.01)a	
	Embryo volume ratio	0.238(0.004)b	0.247(0.003)b	0.280(0.004)a	0.284(0.005)a	
Single seed scan ^d	Seed solid phase volume (mm ³)	2.94(0.25)a	2.52(0.19)a	3.04(0.27)a	2.34(0.36)a	
	Seed Density (g/cm ³)	whole seed	1.33(0.05)a	1.37(0.02)a	1.32(0.01)a	1.40(0.01)a
		Pericarp	2.51(0.04)a	2.38(0.13)a	2.47(0.04)a	2.47(0.04)a
		Embryo	1.47(0.07)a	1.57(0.03)a	1.56(0.01)a	1.51(0.01)a
		Perisperm	1.17(0.05)b	1.19(0.02)ab	1.11(0.01)b	1.27(0.01)a
	Volume ratio	Pericarp	0.058(0.006)ab	0.066(0.002)a	0.061(0.006)ab	0.048(0.004)b
		Embryo	0.259(0.007)a	0.266(0.017)a	0.287(0.014)a	0.298(0.009)a
		Perisperm	0.681(0.009)a	0.666(0.020)a	0.65(0.012)a	0.652(0.008)a
	Weight ratio	Pericarp	0.111(0.014)a	0.115(0.003)a	0.114(0.01)a	0.085(0.007)a
		Embryo	0.286(0.012)b	0.305(0.021)ab	0.340(0.019)a	0.321(0.010)ab
		Perisperm	0.601(0.017)a	0.579(0.022)ab	0.545(0.015)b	0.592(0.011)ab

^a DW = dry weight.

^b From three replicate measures.

^c Thirty seeds sample.

^d Three seeds sample.

the single seed scans. From these scans acquired at high resolution (2 μm voxel size), it was possible to take into account for cavities between the seed parts and then to segment exactly the only solid phase of the seed and to measure its volume. Its average value was highest for Altiplano (3.04 mm^3), followed by Titicaca (2.94 mm^3), Regalona (2.52 mm^3) and Pasankalla (2.34 mm^3). The volume of the voids in the seeds was higher in Altiplano (0.39 mm^3) and Pasankalla (0.38 mm^3) than in Regalona (0.33 mm^3) and Titicaca (0.27 mm^3).

The seed density of the whole seeds determined from the single seed scans was calculated from the ratio of the weights of the three seeds scanned separately and their solid phase volumes. Also this seed density was highest in Pasankalla, followed by Regalona, Titicaca and Altiplano.

The seed part with highest density was the pericarp, followed by the embryo and the perisperm, as is possible to note also from their image gray values (Fig. 1b). In particular, the pericarp density was highest in Titicaca, equal in Altiplano and Pasankalla and lowest in Regalona. The embryo density was the same for Regalona and Altiplano, lower for Pasankalla and lowest for Titicaca. The genotype with highest perisperm density was Pasankalla, while that with the lowest one was Altiplano.

In the following the volumetric ratios will be indicated as embryo ratio, perisperm ratio and pericarp ratio, while the weight ratios will be indicated as embryo W ratio, perisperm W ratio and pericarp W ratio.

The pericarp volume and weight ratios were both highest for Regalona, followed by Altiplano, Titicaca and Pasankalla. The embryo ratio was highest in Pasankalla than in Altiplano, while the embryo W ratio was highest in Altiplano than in Pasankalla, followed in both cases by Regalona and Titicaca. The perisperm volume and weight ratios were highest in Titicaca followed by Regalona, Pasankalla and Altiplano.

The pericarp thickness distribution for the four quinoa genotypes is shown in Fig. 2c. For each genotype, the average pericarp volume of three different thickness classes and the respective standard errors are reported. In Fig. 2a and 2b the pericarp thickness classes are represented in three different colors. In particular, the volumes of pericarp of thickness less than or equal to 15 μm , between 15 and 30 μm and equal or greater than 30 μm were reported in green, yellow and red, respectively. For the class of thickness less than or equal to 15 μm the lowest pericarp volume was observed in the Regalona genotype, while the highest and similar volumes were observed in Altiplano and Pasankalla. The genotypes did not differ significantly from each other. For the intermediate thickness class the pericarp volume was highest in Regalona, followed by Altiplano and Titicaca. Pasankalla showed the lowest volume, which was significantly different from that of the other genotypes. For the upper or equal 30-micron-thickness class, Altiplano showed the largest volume, followed by Titicaca and Regalona with similar values, while in Pasankalla the volume of pericarp thicker than 30 μm was markedly lower. In this latter range, which refers to the largest pericarp thickness, the difference between Altiplano and Pasankalla was significant.

3.4. Principal component analysis

Two PCAs were performed separately with the morpho-densitometric parameters determined from the bulk seed scans and the single seed scans. In Fig. 3 the component loadings and component scores of the PCAs performed on the data from bulk seed scan (Fig. 3a) and single seed scan (Fig. 3b) are shown. In Tables 2 and 3 the resulting Pearson correlation coefficients between the traits as derived from bulk and single seed scans, respectively, are reported. In this work, it was preliminarily decided to consider well-correlated traits if exhibiting coefficient values higher than 0.9 and with a P-value lower than 0.1, thus rejecting the hypothesis of lack of correlation with a significance level of 10%. Since the resolution of the bulk scan allowed only the embryo to be segmented and measured, only the protein content results were

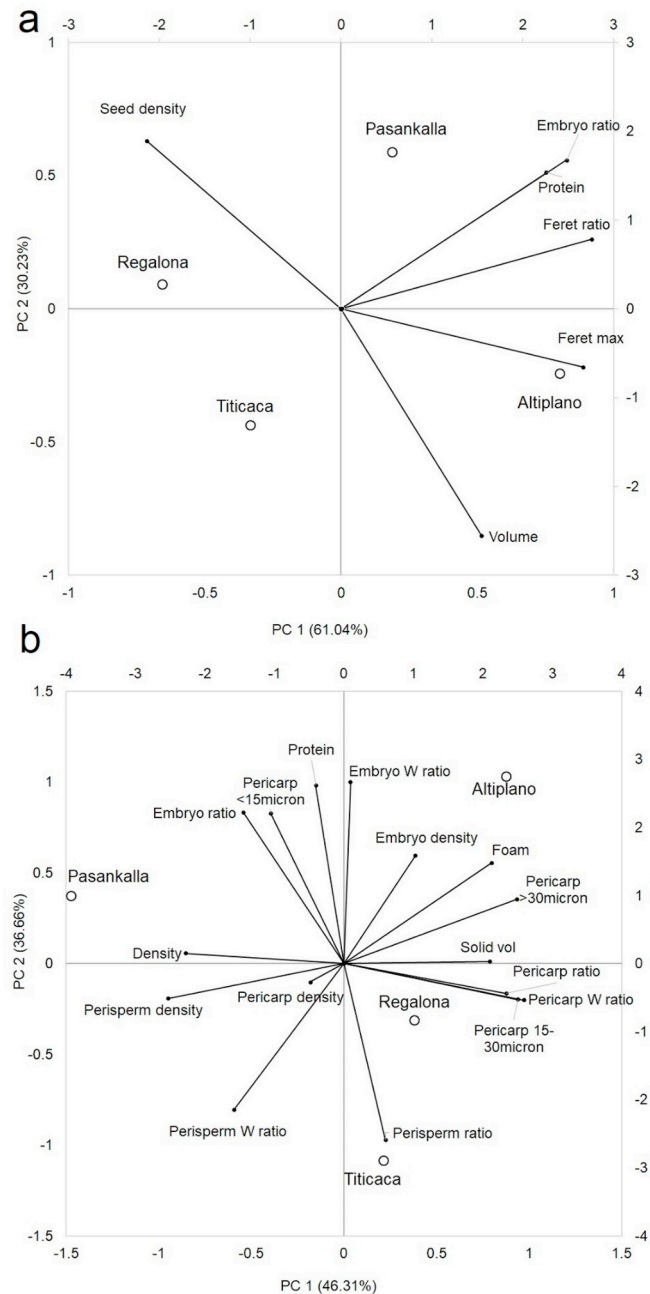


Fig. 3. Principal component analysis (PCA) biplots. Component loadings (black points) represent the quinoa phenotypic traits. Component scores (white circles) of the four genotypes refer to the secondary axes. (a) Results considering morphometric traits from bulk seed scans and the protein content. (b) Results including data from single seed scans along with the protein content and the foam height.

included in the PCA in this case. While in the PCA with single seed scan data the protein content and also the foam height were included.

It can be noted that the embryo ratios reported in Fig. 3a and 3b are different parameters, because in the first case it was calculated referring to the total seed volume, while in the single seed scan measurements all the volume ratios were calculated referring to the seed solid phase volume.

The first two major components of the analysis accounted for 91.27% and 82.97% of the total variation of data in the PCA biplot shown in Fig. 3a and 3b, respectively.

From the PCA biplot shown in Fig. 3a and from Table 2 it was

Table 2
Correlation coefficients among protein content and 5 morphometric traits determined from bulk seed scans.

	Volume (mm ³)	Feret max (mm)	Feret ratio	Seed density (g/cm ³)	Embryo ratio
Protein (% by DW ^a)	-0.015	0.389	0.703	-0.341	0.934*
Volume (mm ³)		0.615	0.230	-0.930*	-0.043
Feret max (mm)			0.878	-0.650	0.587
Feret ratio				-0.402	0.888
Seed density (g/cm ³)					-0.258

^aDW = dry weight, * = $P \leq 0.1$.

possible to observe a high correlation between the protein content and the embryo ratio (correlation coefficient 0.934). Also the correlation coefficient between embryo ratio and Feret ratio was rather high (0.888).

Moreover it can be noted a high negative correlation (-0.930) between the seed density and the total volume of the seed.

From Fig. 3b it can be noted that the protein content results positively correlated with embryo ratio and embryo weight ratio. In particular, as reported in Table 3, the correlation coefficient between the protein content and the embryo weight ratio (0.973) was higher than that between protein content and embryo volume ratio (0.885). The latter correlation coefficient was also lower than that between protein content and embryo volume ratio as obtained from the bulk seed scans, due also to the different parameter definition.

The foam height was positively correlated (0.957) with the volume percentage of pericarp thicker than 30 μm . Thus, among the different pericarp thickness classes, the saponin content best correlated with the amount of pericarp of thickness exceeding 30 μm .

The solid phase seed volume showed a high negative correlation (-0.990) with the seed density. The seed density was positively correlated with the density of the perisperm, which in turn was negatively correlated (-0.903) with the seed solid phase volume.

The pericarp ratio was positively correlated with the pericarp W ratio (0.940). The perisperm ratio was negatively correlated (-0.918) with the embryo ratio and with the embryo W ratio (-0.960).

The volume of pericarp of 15–30 μm thickness was positively correlated with the pericarp W ratio (0.986) and with the pericarp ratio (0.983).

4. Discussion

The PCA in Fig. 3a and the results in Table 2, obtained applying the bulk scan approach of quinoa seeds, allow to confirm the localization of the proteins mainly in the embryo. More in detail, the results in Fig. 3b and Table 3 show that among the many measured morpho-densitometric parameters, the embryo weight ratio presented the highest positive correlation with the protein content (0.973), followed by the embryo volume ratio determined by the bulk seed scans (0.934), being correlations both significant. Thus, an increased embryo size could be a target trait of interest in quinoa breeding programs for the development of improved varieties with higher protein content.

The foam height, and thus the saponin content, correlated with the pericarp portion of thickness exceeding 30 μm . This result confirmed the link between the presence or absence of saponins and the seed coat thickness reported in Jarvis et al. (2017). However, in this latter work, the thickness between the inner and outer layers of the seed coat was measured only locally from two dimensional scanning electron microscopy images. On the contrary, given the irregular and non-uniform structure of the pericarp, the three-dimensional approach used in this work allowed to obtain a complete measurement of the whole pericarp volume and to classify and quantify the volume of portions with different thickness. In particular, the high correlation between foam height and pericarp volume fraction thicker than 30 μm seems to confirm the presence of saponins mainly in the globose cells of the pericarp, which are the largest ones forming the pericarp.

The quite high positive (0.888) and almost significant ($P = 0.112$) correlation between embryo ratio and Feret ratio suggests that the more flat the seed shape is, the higher the ratio between embryo volume and total seed volume is. On the other hand, the Feret ratio has a certain correlation (0.703) also with the protein content, although from our data such correlation is not significant ($P = 0.297$). This means that also such a simple parameter based on the external shape of the seed could give a first indication to predict different protein content for a given genotype with respect to another one. Therefore, the Feret ratio could be considered as a trait for high throughput phenotyping or could be suggested as first seed-sorting criterion for automatic breeding oriented to maximize the protein content. However, further studies on much more genotypes could be needed in order to obtain significant results, which would confirm the above hypothesis. The high negative correlation (-0.93) between the seed density and the total volume of the seed indicate that the mass of a seed tended to remain stable among the quinoa seeds. Thus, there was a greater variability of volume than mass of the seeds. This correlation was also confirmed by the PCA on the single seed scan data where the seed density was calculated referring to the volume only of the solid phase. Moreover, since the perisperm was the volumetrically bigger part of the seed, the high positive correlation between the seed density and the perisperm density could mean that the perisperm is the seed part which mostly influences the variability of the seed density.

Regarding to the comparison of saponin content between the examined quinoa genotypes, based on the classification reported by Koziol (1991) according to which quinoa grains producing foam heights of 1.0 cm or less could be considered sweet, only Pasankalla can be classified as sweet genotype, while Altiplano, Titicaca and Regalona were bitter genotypes. In this regard although inherent limitations of the method could derive from the different properties of specific saponins, Escribano et al. (2017) showed that the varieties with higher amount of saponins after a HPLC/TOF analysis were identified as bitter varieties by the afrosimetric method. Moreover, it allowed a quick estimation of the overall saponins content and the classification of the grains as sweet (low saponins content) or bitter (high saponins content).

In general, the results provided here firstly demonstrate the large amount of morpho-densitometric traits obtainable with X-ray micro-CT imaging on quinoa seeds, with information particularly abundant and detailed when using the single seed scanning approach. The bulk scan approach can actually provide less measurements of seed traits but, as it allows the scanning of hundreds of seeds in one time, it returns clear advantages for representativeness and statistical significance of the results; moreover it is much less time consuming in terms of data processing and analysis allowing to approximate a high throughput phenotyping approach. However, if a trait based on pericarp measurements is required, the single seed scanning remains the mandatory approach.

5. Conclusions

From a methodological perspective, this study shows, with an example on four genotypes, the morpho-densitometric traits that two different X-ray micro-CT scanning approaches (bulk seed and single seed scanning) can provide for quinoa seed deep phenotyping.

Among the novel morpho-densitometric traits measured on quinoa

Table 3
Correlation coefficients among protein content, foam height and 12 morpho-densitometric traits determined from single seed scans.

Traits	Foam height (cm)	Seed solid phase volume (mm ³)	Seed density (g/cm ³)	Pericarp density (g/cm ³)	Embryo density (g/cm ³)	Perisperm density (g/cm ³)	Pericarp ratio	Embryo ratio	Perisperm ratio	Pericarp W ^b ratio	Embryo W ^b ratio	Perisperm W ^b ratio	Volume of pericarp < 15 μm (%)	Volume of pericarp 15–30 μm (%)	Volume of pericarp > 30 μm (%)	
Protein content (% by DW ^a)	0.393	-0.184	0.248	-0.193	0.611	-0.013	-0.240	0.885	-0.997**	-0.332	0.973**	-0.704	0.822	-0.302	0.196	
Foam height (cm)		0.782	-0.775	0.035	0.465	0.923*	0.499	0.055	-0.335	0.634	0.585	0.904*	0.241	0.570	0.957**	
Seed solid phase volume			0.990**	0.460	-0.127	0.903*	0.411	-0.350	0.226	0.690	0.048	-0.442	-0.054	0.562	0.784	
Seed density (g/cm ³)				-0.354	0.068	0.930*	-0.528	0.455	-0.297	-0.782	0.019	0.434	0.178	-0.669	-0.817	
Pericarp density (g/cm ³)					-0.821	-0.053	-0.583	0.122	0.155	-0.271	-0.094	0.243	0.379	-0.426	-0.131	
Embryo density (g/cm ³)						-0.302	0.557	0.208	-0.559	0.337	0.597	-0.744	0.057	0.442	0.515	
Perisperm density (g/cm ³)							-0.689	0.329	-0.052	-0.855	-0.228	0.703	0.116	-0.782	-0.972**	
Pericarp ratio								-0.664	0.312	0.940*	-0.141	-0.413	-0.663	0.983**	0.726	
Embryo ratio									-0.918*	-0.710	0.814	-0.340	0.947*	-0.706	-0.204	
Perisperm ratio										0.403	-0.960**	0.651	-0.851	0.375	-0.126	
Pericarp W* ratio											-0.170	-0.421	-0.598	0.986**	0.826	
Embryo W* ratio												-0.823	0.818	-0.169	0.387	
Perisperm W* ratio													-0.408	-0.413	-0.833	
Volume of pericarp < 15 μm (%)														-0.647	-0.045	
Volume of pericarp 15–30 μm (%)																0.784

^a DW = dry weight, ^bW = weight, * = P ≤ 0.1, ** = P ≤ 0.05.

seeds, the embryo volume and weight ratios derived from the bulk and single seed scanning, respectively, correlated (positively) the best with the protein content, while the pericarp volume fraction of thickness larger than 30 μm was the trait that best correlated (positively) with the saponin amount.

The bulk seed scanning approach showed, overall, the potential for a near high-throughput determination of some novel three-dimensional phenotypic traits of quinoa seeds. In this work 30 seeds for each genotype were analyzed, but potentially also 250 seeds could be acquired in one scan. In particular, such approach could be used on a high number of seeds of different genotypes in order to rapidly obtain a high number of three-dimensional morphometric parameters to be used for identification of the geographic origin of different varieties through a multivariate statistical analysis, enhancing that was done by Medina et al. (2010) using two-dimensional image analysis. Moreover, the morphometric parameters determined with this approach could also be used for improving the technologies associated with the post-harvest processes, to which the quinoa seeds are subjected (Vilche et al., 2003). The bulk seed scanning set up can be straightforwardly used for other types of grains with size similar to quinoa (e.g. amaranth, millet, chia, etc.).

The single seed scanning approach was the only of evaluated methods that was suitable for the three-dimensional characterization of the pericarp structure and for the determination of the densitometric parameters of the different seed tissues. In particular, the used approach allowed to obtain, for each genotype, the pericarp thickness distribution, which entirely characterizes the complex structure of the pericarp with inedited accuracy.

Therefore, depending on the objective of the study, the bulk seed scanning or the single seed scans can be used. The first approach should be when the representativeness of the results and time saving for the analyses are the main goals, the second one when the aim is to characterize at high resolution the morphometry and the density of the different tissues of the seeds.

Acknowledgement

The work for this study has been undertaken as part of the project PROTEIN2FOOD. This project has received funding from the European Union's Horizon 2020 research and innovation programme (grant agreement No 635727).

Appendix A. Supplementary data

Supplementary data to this article can be found online at <https://doi.org/10.1016/j.jcs.2019.102829>.

References

- Abderrahim, F., Huanatico, E., Segura, R., Arribas, S., Gonzalez, M.C., Condezo-Hoyos, L., 2015. Physical features, phenolic compounds, betalains and total antioxidant capacity of colored quinoa seeds (*Chenopodium quinoa* Willd.) from Peruvian Altiplano. *Food Chem.* 183, 83–90. <https://doi.org/10.1016/j.foodchem.2015.03.029>.
- Altuntas, E.A., Naneli, I., Sakin, M.A., 2018. Some selected engineering properties of seven genotypes in quinoa seeds. *Adv. Agric. Sci.* 6, 36–49.
- Ando, H., Chen, Y.-C., Tang, H., Shimizu, M., Watanabe, K., Mitsunaga, T., 2002. Food components in fractions of quinoa seed. *Food Sci. Technol. Res.* 8, 80–84. <https://doi.org/10.3136/fstr.8.80>.
- Bazile, D., Jacobsen, S.-E., Verniau, A., 2016. The global expansion of quinoa: trends and limits. *Front. Plant Sci.* 7, 622. <https://doi.org/10.3389/fpls.2016.00622>.
- Bush, L., Workman, J., Chasse, J., Delonas, C., 2005. Attenuation of X-Rays by matter. *Spectroscopy* 20 (9) Sep 01, 2005. <http://www.spectroscopyonline.com/tutorial-attenuation-x-rays-matter>.
- Carvalho, M.L.M. de, Aelst, A.C.van, Eck, J.W.van, Hoekstra, F.A., 1999. Pre-harvest stress cracks in maize (*Zea mays* L.) kernels as characterized by visual, X-ray and low temperature scanning electron microscopical analysis: effect on kernel quality. *Seed Sci. Res.* 9, 227–236. <https://doi.org/10.1017/S0960258599000239>.
- Escribano, J., Cabanes, J., Jiménez-Atiénzar, M., Ibañez-Tremolada, M., Gómez-Pando, L.R., García-Carmona, F., Gandía-Herrero, F., 2017. Characterization of betalains, saponins and antioxidant power in differently colored quinoa (*Chenopodium quinoa*)

- varieties. *Food Chem.* 234, 285–294. <https://doi.org/10.1016/j.foodchem.2017.04.187>.
- FAO, CIRAD, 2015. In: Bazile, D., Bertero, D., Nieto, C. (Eds.), *State of the Art Report of Quinoa in the World in 2013*, (Rome).
- Fuentes, F., Paredes-Gonzales, X., 2015. Nutraceutical perspectives of quinoa: biological properties and functional applications. Chapter XX. In: *FAO & CIRAD. State of the Art Report of Quinoa in the World in 2013*, pp. 286–299 (Rome).
- Guelpa, A., du Plessis, A., Kidd, M., Manley, M., 2015. Non-destructive estimation of maize (*Zea mays* L.) kernel hardness by means of an X-ray micro-computed tomography (μCT) density calibration. *Food Bioprocess Technol.* 8, 1419–1429. <https://doi.org/10.1007/s11947-015-1502-3>.
- Gustin, J.L., Jackson, S., Williams, C., Patel, A., Armstrong, P., Peter, G.F., Settles, A.M., 2013. Analysis of maize (*Zea mays*) kernel density and volume using microcomputed tomography and single-kernel near-infrared spectroscopy. *J. Agric. Food Chem.* 61, 10872–10880. <https://doi.org/10.1021/jf403790v>.
- Hinojosa, L., González, J.A., Barrios-Masias, F.H., Fuentes, F., Murphy, K.M., 2018. Quinoa abiotic stress responses: a review. *Plants* 7 (4), 106. <https://doi.org/10.3390/plants704106>.
- Jacobsen, S.-E., 2017. The scope for adaptation of quinoa in Northern Latitudes of Europe. *J. Agron. Crop Sci.* 203, 603–613. <https://doi.org/10.1111/jac.12228>.
- Jarvis, D.E., Ho, Y.S., Lightfoot, D.J., Schmöckel, S.M., Li, B., Borm, T.J.A., Ohyanagi, H., Mineta, K., Michell, C.T., Saber, N., Kharbatia, N.M., Rupper, R.R., Sharp, A.R., Dally, N., Boughton, B.A., Woo, Y.H., Gao, G., Schijlen, E.G.W.M., Guo, X., Momin, A.A., Negrão, S., Al-Babili, S., Gehring, C., Roessner, U., Jung, C., Murphy, K., Arold, S.T., Gojbori, T., Linden, C.G.van der, van Loo, E.N., Jellen, E.N., Maughan, P.J., Tester, M., 2017. The genome of *Chenopodium quinoa*. *Nature* 542, 307–312. <https://doi.org/10.1038/nature21370>.
- Kozioł, M.J., 1991. Afrosimetric estimation of threshold saponin concentration for bitterness in quinoa (*Chenopodium quinoa* Willd.). *J. Sci. Food Agric.* 54, 211–219. <https://doi.org/10.1002/jsfa.2740540206>.
- Liu, Q., Liu, H., Zhang, L., Guo, T., Wang, P., Geng, M., Li, Y., 2013. Synthesis and antitumor activities of naturally occurring oleoanolic acid triterpenoid saponins and their derivatives. *Eur. J. Med. Chem.* 64, 1–15. <https://doi.org/10.1016/j.ejmech.2013.04.016>.
- Medina, W., Skurtys, O., Aguilera, J.M., 2010. Study on image analysis application for identification Quinoa seeds (*Chenopodium quinoa* Willd.) geographical provenance. *LWT - Food Sci. Technol. (Lebensmittel-Wissenschaft -Technol.)* 43, 238–246. <https://doi.org/10.1016/j.lwt.2009.07.010>.
- Prado, F.E., Fernández-Turiel, J.L., Tsarouchi, M., Psaras, G.K., González, J.A., 2014. Variation of seed mineral concentrations in seven quinoa cultivars grown in two agroecological sites. *Cereal Chem. J.* 91, 453–459. <https://doi.org/10.1094/CCHEM-08-13-0157-R>.
- Prego, I., Maldonado, S., Otegui, M., 1998. Seed structure and localization of reserves in *Chenopodium quinoa*. *Ann. Bot.* 82, 481–488. <https://doi.org/10.1006/anbo.1998.0704>.
- Reguera, M., Conesa, C.M., Gil-Gómez, A., Haros, C.M., Pérez-Casas, M.Á., Briones-Labarca, V., Bolaños, L., Bonilla, I., Álvarez, R., Pinto, K., Mujica, Á., Bascuñán-Godoy, L., 2018. The impact of different agroecological conditions on the nutritional composition of quinoa seeds. *PeerJ* 6, e4442. <https://doi.org/10.7717/peerj.4442>.
- Rizvi, M.A., Ali, S.A., Munir, I., Yasmeen, K., Abid, R., Ahmed, S., 2017. Cultivation of new emerging agro-nutritional crop of quinoa at Madinat al-Hikmah Karachi, Sindh, Pakistan. *Open Plant Sci. J.* 10, 70–81. <https://doi.org/10.2174/1874294701710010070>.
- Ruiz, K.B., Khakimov, B., Engelsens, S.B., Bak, S., Biondi, S., Jacobsen, S.-E., 2017. Quinoa seed coats as an expanding and sustainable source of bioactive compounds: an investigation of genotypic diversity in saponin profiles. *Ind. Crops Prod.* 104, 156–163. <https://doi.org/10.1016/j.indcrop.2017.04.007>.
- Takhar, P.S., Maier, D.E., Campanella, O.H., Chen, G., 2011. Hybrid mixture theory based moisture transport and stress development in corn kernels during drying: validation and simulation results. *J. Food Eng.* 106, 275–282. <https://doi.org/10.1016/j.jfoodeng.2011.05.006>.
- Van Raamsdonk, L.W.D., Pinckaers, V., Ossenkoppele, J., Houben, R., Lotgering, M., Groot, M.J., 2010. Quality assessments of untreated and washed quinoa (*Chenopodium quinoa*) seeds based on histological and foaming capacity investigations. In: *Microscopy: Science, Technology, Applications and Education*. Formatex Research Center.
- Vilche, C., Gely, M., Santalla, E., 2003. Physical properties of quinoa seeds. *Biosyst. Eng.* 86, 59–65. [https://doi.org/10.1016/S1537-5110\(03\)00114-4](https://doi.org/10.1016/S1537-5110(03)00114-4).
- Wimalasekera, R., 2015. Role of seed quality in improving crop yields. In: *Crop Production and Global Environmental Issues*. Springer International Publishing, Cham, pp. 153–168. https://doi.org/10.1007/978-3-319-23162-4_6.
- Wu, G., Peterson, A.J., Morris, C.F., Murphy, K.M., 2016. Quinoa seed quality response to sodium chloride and sodium sulfate salinity. *Front. Plant Sci.* 7, 790. <https://doi.org/10.3389/fpls.2016.00790>.
- Xiao, S., Bresler, Y., Munson, D.C., 2003. Fast Feldkamp algorithm for cone-beam computer tomography. In: *Proceedings 2003 International Conference on Image Processing (Cat. No.03CH37429)*, pp. 81–89. <https://doi.org/10.1109/ICIP.2003.1246806>. Barcelona, Spain, 2003.
- Yao, Y., Yang, X., Shi, Z., Ren, G., 2014. Anti-inflammatory activity of saponins from quinoa (*Chenopodium quinoa* Willd.) seeds in lipopolysaccharide-stimulated RAW 264.7 Macrophages Cells. *J. Food Sci.* 79, H1018–H1023. <https://doi.org/10.1111/1750-3841.12425>.
- Zurita-Silva, A., Fuentes, F., Zamora, P., Jacobsen, S.-E., Schwember, A.R., 2014. Breeding quinoa (*Chenopodium quinoa* Willd.): potential and perspectives. *Mol. Breed.* 34, 13–30. <https://doi.org/10.1007/s11032-014-0023-5>.